ISSN 1063-7796, Physics of Particles and Nuclei, 2015, Vol. 46, No. 5, pp. 740–745. © Pleiades Publishing, Ltd., 2015.

Recent Results from High Temperature Lattice QCD[1]

E. Laermann
Fakultät für Physik, Universität Bielefeld, D-33615 Bielefeld, Germany
e-mail: edwin@physik.uni-bielefeld.de

Abstract—Recent results obtained from numerical computations in lattice regularized QCD are summarized. The write-up of the talk concentrates on the liberation of strange quarks in the vicinity of the chiral QCD transition and on certain ratios of cumulants of net electric charge fluctuations which can be used to determine freeze-out parameters by a comparison of experimental data from heavy ion collisions with lattice QCD results.

DOI: 10.1134/S1063779615050147

1. INTRODUCTION

Fluctuations and correlations of conserved charges like baryon number B, electric charge Q or strangeness S are sensitive to the composition of hot and dense QCD matter [1, 2]. Measures of them in general take quite different values in a phase where the carriers of the quantum numbers are hadrons opposed to a phase where those are quarks. It is therefore of interest to compute fluctuation and correlation quantities from QCD to study the properties of strong-interaction matter at high temperature and density.

Moreover, fluctuations measured in a heavy ion collision experiment may reflect thermal conditions at the time where the generated medium has expanded, cooled down and diluted sufficiently so that hadrons form again. Although it may be questioned whether the thermal medium at this time is in equilibrium and how well hadronization is localized in time, the success of hadron resonance gas (HRG) model calculations, performed to describe properties of the medium at the time of freeze-out [3], seems to suggest that the thermal conditions are well characterized by a freeze-out temperature T_f and a baryon chemical potential μ_B^f. The values T_f and μ_B^f at freeze-out are usually determined by comparing experimental data on particle yields with a HRG model calculation [3, 4]. However, it clearly is desirable to extract the freeze-out parameters also by comparing experimental data directly with a QCD calculation.

In the following write-up of the talk I will concentrate on strangeness liberation and on determining freeze-out parameters with the help of lattice QCD. Both topics rely on our measurements of fluctuation and correlation variables performed for two degenerate light quarks and a strange quark. The quark mass values have been tuned such that the Kaon mass acquires its physical value and that the (Goldstone) pion is of mass 160 MeV. The simulations are based on the socalled hisq action [5] for the quarks, a highly improved discretization with small discretization errors (taste violations). At aspect ratios $N_\sigma/N_\tau \geq 4$, the temporal extents of the $N_\sigma^3 \times N_\tau$ lattices have been chosen as $N_\tau = 6$, 8 and 12 to address finite lattice spacing effects $\sim(N_\tau T)^{-1}$ with T being the temperature.

2. STRANGENESS LIBERATION

The basic quantities calculated on the lattice arise from a Taylor expansion of the pressure, or equivalently of the logarithm of the partition function,

$$\frac{p}{T^4} = \frac{1}{VT^3}\ln Z(T, \mu_u, \mu_d, \mu_s)$$
$$= \sum_{i,j,k}\frac{1}{i!j!k!}\chi_{ijk}(T)\left(\frac{\mu_u}{T}\right)^i\left(\frac{\mu_d}{T}\right)^j\left(\frac{\mu_s}{T}\right)^k,$$

with respect to the quark chemical potentials $\mu_{u,d,s}$. The expansion coefficients χ_{ijk} are computed at vanishing chemical potentials and are readily combined into generalized susceptibilities[2] χ_{ijk}^{BQS} which are related to correlations between the conserved quantum numbers B, Q and S as well as to cumulants of fluctuations like e.g. variance, skewness or kurtosis.

The generalized susceptibilities can also be obtained in hadron resonance gas model calculations. In a HRG picture the contribution to the partition

[1] The article is published in the original.

[2] Whenever a subscript is zero it will be omitted as is the corresponding superscript.

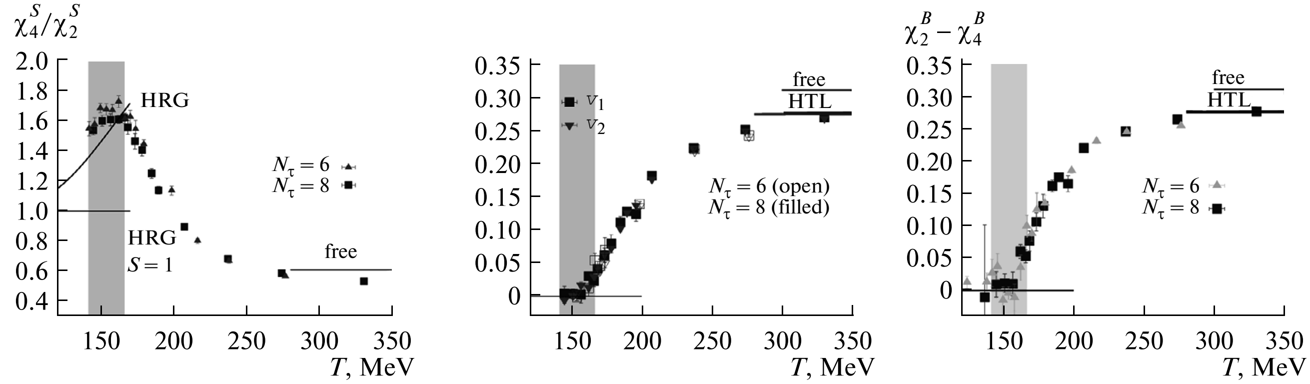

Fig. 1. The quantities χ_4^S/χ_2^S (left), v_1 and v_2 of Eq. (3) (middle) and $\chi_2^B - \chi_4^B$ (right) as a function of temperature. The grey bands indicate the chiral transition region.

function Z of a meson (M) or a baryon (B) with quantum numbers and mass indexed by i is given by

$$\ln Z_i^{M/B} \sim \sum_{k=1}^{\infty} \frac{(\pm 1)^{k+1}}{k^2} K_2(km_i/T) \times \cosh(k(B_i\hat{\mu}_B + Q_i\hat{\mu}_Q + S_i\hat{\mu}_S)) \quad (1)$$

($\hat{\mu}_X = \mu_X/T$, $X = B, Q, S$) such that the total pressure is obtained as a sum over of partial pressures $M_{|S|}$ and $B_{|S|}$ of mesons and baryons resp.,

$$\frac{p}{T^4} = M_0(T) + M_1(T)\cosh(-\hat{\mu}_S) + B_0(T) \times \cosh(\hat{\mu}_B) + B_1(T)\cosh(\hat{\mu}_B - \hat{\mu}_S) + B_2(T) \times \cosh(\hat{\mu}_B - 2\hat{\mu}_S) + B_3(T)\cosh(\hat{\mu}_B - 3\hat{\mu}_S), \quad (2)$$

where for the strange mesons and the baryons the Boltzmann approximation has been applied which is good within 2% accuracy. Taking Eq. (2) as the starting point for HRG computations of χ_{ijk}^{BQS} as appropriate derivatives with respect to the chemical potentials, it is easily seen that in a gas of uncorrelated hadrons $\chi_2^B = \chi_4^B$, for instance, whereas the deviation of χ_4^S from χ_2^S is a measure for the contribution of $|S| > 1$ hadrons. This contribution is shown in Fig. 1 to be quite substantial below the chiral crossover at $T = 154(9)$ MeV [6] indicated as the grey band. At higher temperature though, the ratio of the susceptibilities χ_4^S/χ_2^S rapidly approaches the free quark gas value.

Up to fourth order in the derivative with respect to the strangeness chemical potential, in a hadron resonance gas, Eq. (2), there are 6 generalized susceptibilities, χ_{11}^{BS}, χ_{31}^{BS}, χ_2^S, χ_{22}^{BS}, χ_{13}^{BS} and χ_4^S, but only 4 partial pressures. Thus one can construct 2 independent combinations of the susceptibilities that should vanish in a phase where the B and S quantum numbers are carried by hadrons, e.g.

$$v_1 = \chi_{31}^{BS} - \chi_{11}^{BS},$$
$$v_2 = \frac{1}{3}(\chi_2^S - \chi_4^S) - 2\chi_{13}^{BS} - 4\chi_{22}^{BS} - 2\chi_{31}^{BS}. \quad (3)$$

These quantities are also shown in Fig. 1. As can be seen, v_1 and v_2 are vanishing up to temperatures in the chiral transition range, in accord with the hadron gas scenario, but simultaneously rise rapidly beyond. This rise is comparable in size to the rise in $\chi_2^B - \chi_4^B$ shown in the right part of Fig. 1. This fact shows that the behavior of the strange degrees of freedom is very similar to the one of light quarks. Both sets of quantities are approaching the predictions of re-summed Hard Thermal Loop (HTL) perturbation theory [7] at temperatures of about two times the chiral crossover one.[3]

Solving for the partial pressures $M_{|S|}$ and $B_{|S|}$ arising from the strange hadron sector ($|S| \geq 1$) of an HRG leads to

$$M_1(c_1, c_2) = \chi_2^S - \chi_{22}^{BS} + c_1 v_1 + c_2 v_2,$$
$$B_1(c_1, c_2) = \frac{1}{2}(\chi_4^S - \chi_2^S + 5\chi_{13}^{BS} + 7\chi_{22}^{BS}) + c_1 v_1 + c_2 v_2,$$
$$B_2(c_1, c_2) = -\frac{1}{4}(\chi_4^S - \chi_2^S + 4\chi_{13}^{BS} + 4_{22}^{BS}) + c_1 v_1 + c_2 v_2, \quad (4)$$
$$B_3(c_1, c_2) = \frac{1}{18}(\chi_4^S - \chi_2^S + 3\chi_{13}^{BS} + 3_{22}^{BS}) + c_1 v_1 + c_2 v_2,$$

where arbitrary linear combinations of v_1 and v_2 can be added without affecting; the result. These partial

[3] For a more detailed discussion see [8].

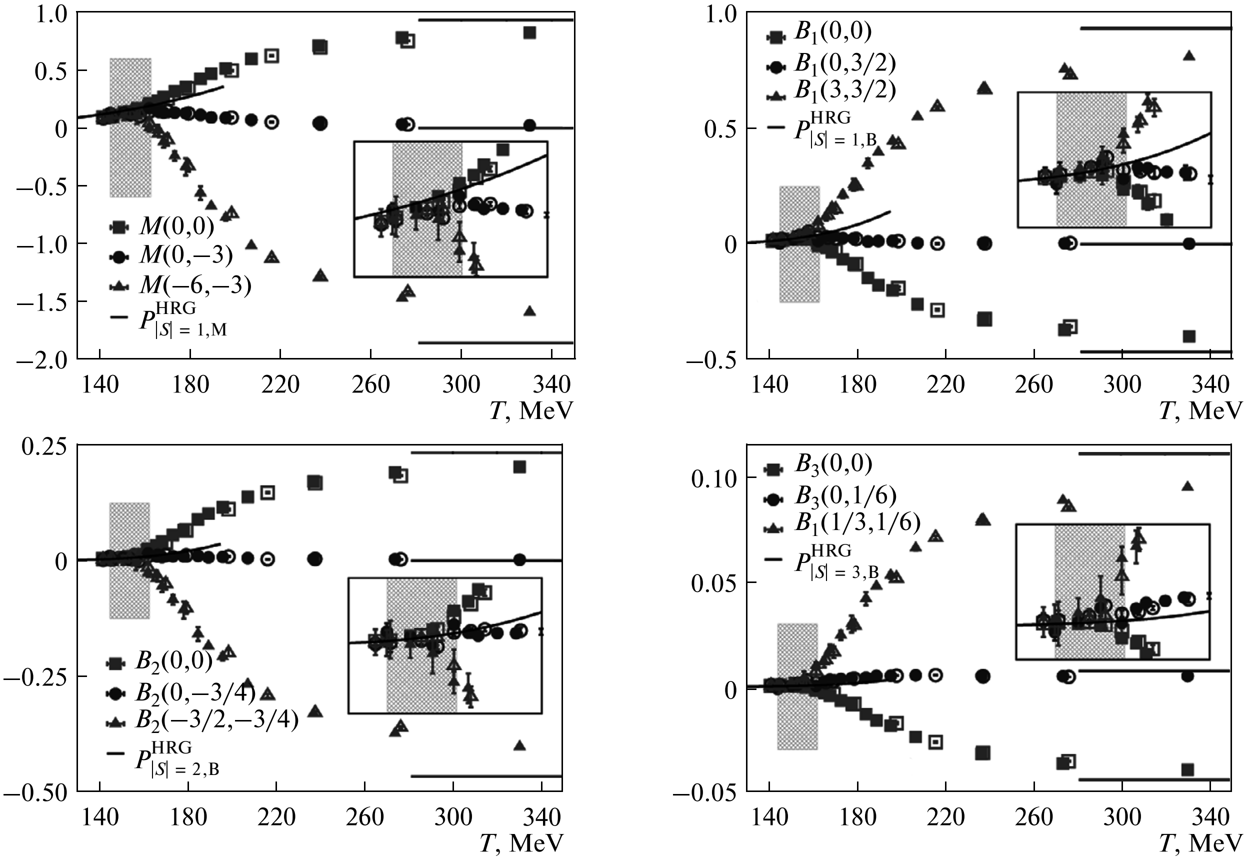

Fig. 2. Partial pressures arising from the strange sector of an HRG, Eq. (4). The yellow bands indicate the chiral transition region, whereas the colored lines on the right side denote the quark gas values.

pressures are shown in Fig. 2. While at low temperatures up to the chiral transition region the various linear combinations agree with each other and with the HRG predictions, the hadronic description of the strange degrees of freedom breaks down just above T_c.

3. FREEZE-OUT PARAMETERS

As mentioned in the previous section, the lattice results for generalized susceptibilities depend on temperature and the chemical potentials μ_B, μ_Q and μ_S. In order to get access to the freeze-out parameters T_f and μ_B^f one needs to fix μ_Q and μ_S to values that characterize a thermal system created in a heavy ion collision. These values are determined by assuming that the thermal sub-volume, probed by measuring fluctuations in a certain rapidity and transverse momentum window, reflects the net strangeness content and electric charge to baryon number ratios of the incident nuclei,

$$\langle n_S \rangle = 0, \quad \langle n_Q \rangle = r \langle n_B \rangle, \tag{5}$$

where r is approximately 0.4 for Au–Au as well as Pb–Pb collisions. Expanding the densities in terms of the chemical potentials one can solve for and μ_S order by order in the expansion, with the result up to next-to-leading order (NLO) as

$$\hat{\mu}_Q = q_1 \hat{\mu}_B + q_3 \hat{\mu}_B^3, \quad \hat{\mu}_S = s_1 \hat{\mu}_B + s_3 \hat{\mu}_B^3. \tag{6}$$

The leading order expansion coefficients for $\hat{\mu}_Q$ and $\hat{\mu}_S$ are shown in the top panels of Fig. 3. Based on spline interpolations of the numerical results obtained for three different lattice sizes, extrapolations to the continuum limit were carried out using an ansatz linear in $1/N_\tau^2$. The resulting extrapolations are shown as bands in these panels. In order to check the importance of NLO corrections, s_3 and q_3 were calculated on lattices with temporal extent $N_\tau = 6$ and 8. The results, expressed in units of the leading order terms, are also shown in Fig. 3. It is obvious from this figure that NLO corrections indeed are negligible in the high temperature region and smaller than 10% in the temperature interval relevant for the analysis of freeze-out conditions, i.e., $T \simeq (160 \pm 10)$ MeV. (For a more detailed discussion of the errors of these and other quantities presented below, I refer to [9].)

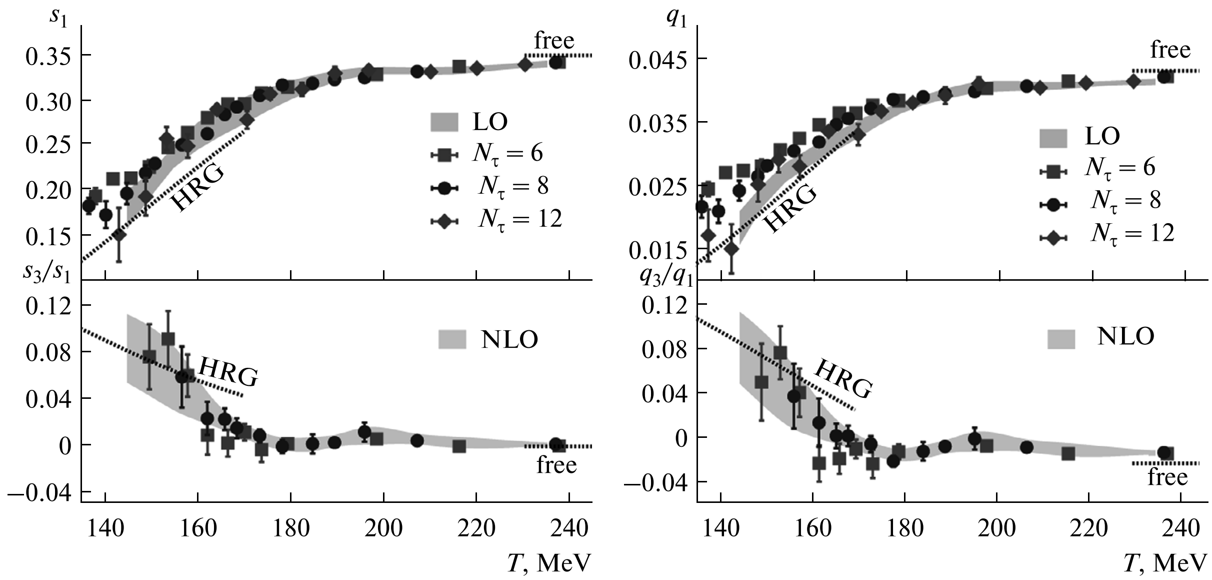

Fig. 3. The leading and next-to-leading order expansion coefficients of the strangeness (left) and the negative of the electric charge chemical potentials (right) versus temperature for $r = 0.4$. For s_1 and q_1 the LO-bands show results for the continuum extrapolation. For s_3 and q_3 we give an estimate for continuum results (NLO bands) based on spline interpolations of the $N_\tau = 8$ data. Dashed lines at low temperature are from the HRG model and at high temperature from a massless, 3-flavor quark gas.

Having thus adjusted the values for μ_Q and μ_S to the physical conditions met in a heavy ion collision, two further quantites are needed to fix T^f and μ_B^f. Of particular interest are ratios of cumulants which to a large extent eliminate the dependence of cumulants on the freeze-out volume. Since only proton instead of baryon fluctuations are available experimentally, electric charge fluctuations appear to be most appropriate. The simplest of such ratios involve mean M_Q, variance σ_Q^2 and skewness S_Q. Those can be combined to

$$\frac{M_Q(s)}{\sigma_Q^2(s)} = \frac{\chi_1^Q(T, \mu_B)}{\chi_2^Q(T, \mu_B)} = R_{12}^Q(T, \mu_B) \tag{7}$$
$$= R_{12}^{Q,1}(T)\hat{\mu}_B + R_{12}^{Q,3}(T)\hat{\mu}_B^3 + \dots,$$

$$\frac{S_Q(s)\sigma_Q^3(s)}{M_Q(s)} = \frac{\chi_3^Q(T, \mu_B)}{\chi_1^Q(T, \mu_B)} = R_{31}^Q(T, \mu_B) \tag{8}$$
$$= R_{31}^{Q,0}(T) + R_{31}^{Q,2}(T)\hat{\mu}_B^2 + \dots.$$

These ratios can be computed in QCD (as well as in the HRG model) and can be compared to experimental data in order to determine T^f and μ_B^f. We evaluated them to leading order for R_{31}^Q and up to $\mathcal{O}(\hat{\mu}_B^3)$ for R_{12}^Q. For the latter case the leading order and the NLO corrections are shown in Fig. 4. The LO results have been obtained on lattices with $N_\tau = 6$, 8 and 12. They show small discretization effects and were extrapolated to the continuum limit. The NLO corrections to the ratio of electric charge cumulants are below 10%, which makes the leading order result a good approximation for a large range of $\hat{\mu}_B$.

The leading part of the ratio R_{12}^Q depends linearly on μ_B such that this ratio has a strong dependence on μ_B but varies little with T for $T \simeq (160 \pm 10)$ MeV, see Fig. 5 (left). On the contrary, to leading order R_{31}^Q depends strongly on T, Fig. 5 (right), and shows a characteristic temperature dependence for $T \gtrsim 155$ MeV that is quite different from that of HRG model calculations. It receives corrections only at $\mathcal{O}(\hat{\mu}_B^2)$ an estimate of which has been added as blueish band in the figure.

The idea is now to compare the lattice results for these ratios, which are functions of T and μ_B, to experimental data at given center-of-mass energy. A measurement of R_{31}^Q lends itself for a determination of the freeze-out temperature, with small values of R_{31}^Q favoring large freeze-out temperatures T^f and vice versa. Subsequently, a comparison of experimental data on R_{12}^Q with Fig. 5 (left) will allow to determine μ_B^f.

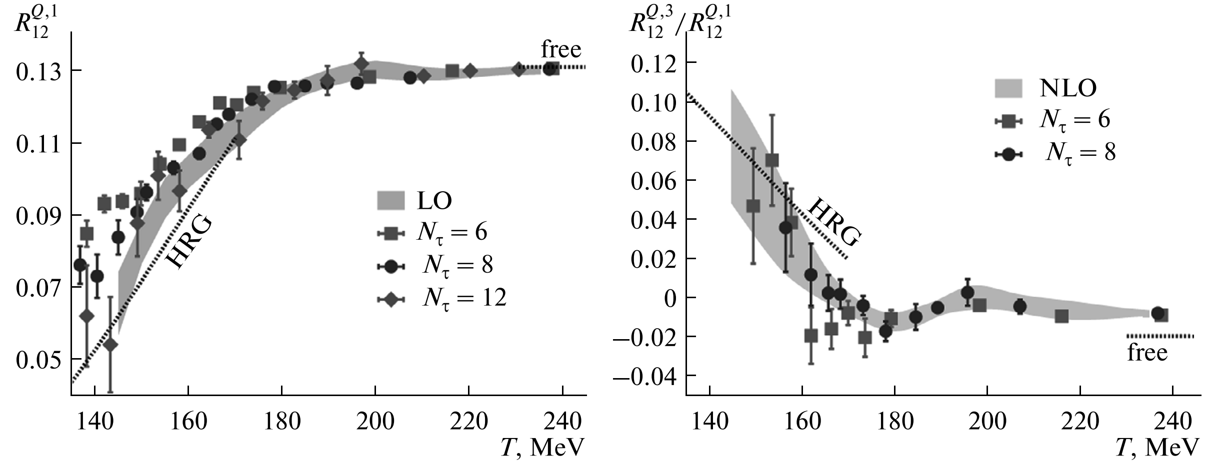

Fig. 4. The leading (left) and next-to-leading (right) order expansion coefficients of the ratio of first to second order cumulants of net electric charge fluctuations versus temperature for $r = 0.4$. The bands and lines are as in Fig. 3.

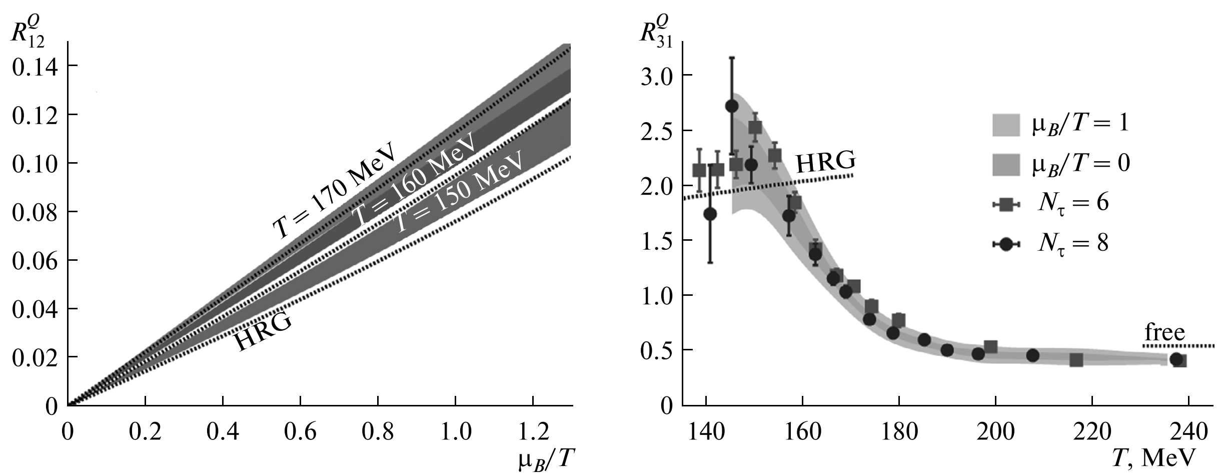

Fig. 5. The ratios R_{12}^{Q} versus μ_B/T (left) for three values of the temperature and R_{31}^{Q} versus temperature for $\mu_B = 0$ (right). The wider band on the data set for $N_\tau = 8$ (right) shows an estimate of the magnitude of NLO corrections at $\mu_B/T = 1$.

4. CONCLUSIONS

The lattice QCD results presented here show that up to the chiral crossover temperature T_c the quantum numbers associated with strange degrees of freedom are consistent with that of an uncorrelated gas of hadrons. The lattice results also show that such a hadronic description breaks down just above T_c. Moreover, the behavior of the strange degrees of freedom around T_c is quite similar to that involving the light up and down quarks, altogether suggesting that the deconfinement of strangeness takes place at the chiral crossover temperature.

Furthermore, the first three cumulants of net electric charge fluctuations are well suited for a determination of freeze-out parameters in a heavy ion collision. Although the ratios R_{12}^{Q} and R_{31}^{Q} are sufficient to determine T_f and μ_B^f, it would be advantageous to have several ratios to probe the consistency of an equilibrium thermodynamic description of freeze-out. When comparing these results to experimental data one will however need to take into account details of the actual experimental set-up. In addition, the thermodynamic relevance of additional, experimentally yet unobserved strange baryons, as observed in the meantime after the Symposium [10], also has consequences for the analysis of freeze-out conditions in heavy ion experiments.

ACKNOWLEDGMENTS

The author thanks the organizers for the outstanding atmosphere at the symposium. The presentation here is based on work within the BNL-Bielefeld collaboration. Partial financial support from the European Union under Grant Agreement number 238353 is acknowledged.

REFERENCES

1. V. Koch, A. Majumder, and J. Randrup, "Baryon-strangeness correlations: A diagnostic of strongly interacting matter," Phys. Rev. Lett. **95,** 182301 (2005).
2. S. Ejiri, F. Karsch, and K. Redlich, "Hadronic fluctuations at the QCD phase transition," Phys. Lett., B **633,** 275 (2006).
3. P. Braun-Munzinger, K. Redlich, and J. Stachel, "Particle production in heavy ion collisions,", in *Quark Gluon Plasma 3, Ed. by R. C. Hwa and X. N. Wang (World Scientific, Singapore, 2004)*, p. 491; [nucl-th/0304013].
4. J. Cleymans et al., "Comparison of chemical freeze-out criteria in heavy-ion collisions," Phys. Rev., C **73,** 034905 (2006).
5. E. Follana et al. (HPQCD and UKQCD Collab.), "Highly improved staggered quarks on the lattice, with applications to charm physics," Phys. Rev., D **75,** 054502 (2007).
6. A. Bazavov et al., "The chiral and deconfinement aspects of the QCD transition," Phys. Rev., D **85,** 054503 (2012).
7. J. O. Andersen, S. Mogliacci, N. Su, and A. Vuorinen, "Quark number susceptibilities from resummed perturbation theory," Phys. Rev., D **87,** 074003 (2013).
8. A. Bazavov et al., "Strangeness at high temperatures: from hadrons to quarks," Phys. Rev. Lett. **111,** 082301 (2013).
9. A. Bazavov et al., "Freeze-out conditions in heavy ion collisions from QCD thermodynamics," Phys. Rev. Lett. **109,** 192302 (2012).
10. A. Bazavov et al., "Additional strange hadrons from QCD thermodynamics and strangeness freeze-out in heavy ion collisions," Phys. Rev. Lett. **113,** 072001 (2014).